Master of Science Thesis in Electrical Engineering
Department of Electrical Engineering, Linköping University, 2020

Alternative Input Devices for Steer-by-Wire Systems

Casper Christiansen and Viktor Alkelin

Master of Science Thesis in Electrical Engineering

Alternative Input Devices for Steer-by-Wire Systems

Casper Christiansen and Viktor Alkelin

LiTH-ISY-EX--20/5296--SE

Supervisor: **Victor Fors**
ISY, Linköpings universitet
Matthijs Klomp
Solution Architect, Volvo Cars

Examiner: **Jan Åslund**
ISY, Linköpings universitet

Division of Vehicular Systems
Department of Electrical Engineering
Linköping University
SE-581 83 Linköping, Sweden

Abstract

With the recent push towards autonomous cars, a traditional steering wheel with its mechanical connection between the road and driver may soon be unnecessary. To facilitate interior design and lower production costs whilst still maintaining a manual alternative for maneuvering, an alternative steering input device relying on Steer-by-Wire technology is investigated.

In order to finish the investigation and development of the steering device within the time-span of a master thesis, the limitation to only investigate the design of a hand wheel was established.

The finished alternative steering device utilises an optical encoder for position measurement and a brushless direct current (DC) motor with a planetary gearbox for force feedback. Open-loop speed control proved to be insufficient with the available hardware. Instead, an approach of two PD-controllers regulating the angular error between the steering rack and the steering device was implemented successfully.

Initially, mathematical models of the system components were derived and implemented in Mathworks Simulink. The transition from models to test rig implementation proved to be difficult due to unknown parameters in the hardware components such as embedded controllers in the steering gear and the internal works of the sensor emulator used to control the steering gear. By modifying parameters in accordance with system identification measurements performed on the test rig, the models could be validated.

At the end of the project, a Volvo S60 was made available and the steering device was tested with real world driving. It was discovered that controllers tuned only for good reference following in the test rig did not translate to good drive-ability as the controller allowed for overly aggressive maneuvers. Following some in vehicle tuning, the proposed solution performed well during testing with surprisingly high drive-ability.

For future iterations of similar hand wheel design projects, a user study was performed with regards to user experience, hand wheel size and perceived drive-ability.

Acknowledgments

We would like to extend our gratitude to Volvo Cars for such an exciting opportunity to test and prove our engineering knowledge.

With special thanks to Matthijs Klomp for his personal interest and guidance in our thesis project, Georgios Minos for the administrative aid and we also want to acknowledge everyone at steering, who helped us answering questions and supplying data.

From Linköpings University we want to thank Victor Fors for all his work improving the quality of our master thesis and Jan Åslund for assuring the academical reach.

Not to be forgotten is Adrian Aune, William Andersson, Axel Jyrkäs, Gustav Ljungquist and Harish Kumar for the good company during our lunches.

Finally, we do not in any way want to thank COVID-19 for all its complications to our thesis work and potential future careers.

Stay safe

Gothenburg, June 2020
Casper Christiansen and Viktor Alkelin

Contents

List of Figures

Notation

Abbreviations

Abbreviation	Meaning
SbW	Steer-by-Wire
PID	Proportional, Integral, Differential (controller)
HID	Human Interface Devices
DC	Direct Current
AC	Alternating Current
BLDC	Brushless Direct Current motor
MIL	Model In the Loop
SIL	Software In the Loop
HIL	Hardware In the Loop
ECU	Electronic Control Unit
EPAS	Electronic Power Assisted Steering
HPAS	Hydraulic Power Assisted Steering
ECU	Electric Control Unit
PSCU	Power Steering Control Unit
EMI	Electromagnetic Interference
SPA	Scalable Product Architecture

1 Introduction

1.1 Introduction

With the current push towards autonomous cars, the need for a large steering wheel with mechanical connection to the road might be slowly diminishing. New innovative solutions that require less space and add more freedom for vehicle interior design may therefore be developed as manual back-ups to the autonomous systems. Former Swedish car manufacturer Saab experimented with a prototype vehicle as a part of the Pan-European project Prometheus which utilized a joystick-type steering device as early as 1992. Although the project never left the research stage, some promising results were found in terms of reported intuitive steering feel after some habituation [1].

Steer-by-Wire (SbW) systems rely on sensors, controllers and motors in order to electronically transmit driver steering input to a motor located on the steering gear assembly in combination with another motor used for providing the driver with road feedback. In comparison, a traditional steering system transmits steering wheel torque mechanically to the steering gear assisted with either electronic power assisted (EPAS) or hydraulic power assisted systems (HPAS). The possible benefits of SbW systems include:

- Space-savings and reduced manufacturing costs
- Facilitate implementation of driver-assistance systems for improved road safety
- Increased vehicle interior design freedom
- Variable input/output steering ratios and feedback in different situations

Still to date, the steering standard in the automotive industry is a mechanical connection between the driver and the wheels, despite a long history of extensive research about SbW systems [2]. The main problem leading to the slow adoption of by-Wire technology is the strict safety regulations regarding the lack of a mechanical connection between the steering wheel and steering gear, which requires new implementations of system redundancies and various fail-safe procedures [3]. Autonomous cars drive a new revolution in terms of offsetting the high cost and complexity of these systems weighed against customer value as SbW technology is a must for driverless cars [4].

1.2 Problem description

The main objective of this thesis is to investigate the implementation of an alternative input device for SbW systems from a control theoretical view-point. This will be performed by analysing the differences between simulated system to test rig and eventually real car implementation. The work is conducted together with Volvo Cars, so the vehicle implementation will relate to a Volvo.

The following list describes the thesis problem formulation:

1. How can a SbW system for an alternative steering device be modelled and implemented?
2. Which control performance indicators of such SbW system are most effected by implementation in a passenger vehicle?
3. What cost-effective alternatives of redundancy are applicable to the realisation of the system?

The main requirements of the vehicle implementation is described below:

- Provide a solution for manual steering in autonomous cars
- Minimal space-usage and no permanent modification to the vehicle
- Should be able to handle parking and relatively low speed maneuvers safely

To validate the vehicle implementation, a user-study will be performed with the finished prototype.

1.3 Approach

The thesis approach is divided into the following stages:

1. Literature review on relevant topics
2. System modelling and tuning
3. System prototyping and implementation
4. Validation, comparison and conclusion

When the first stage of literature review is completed, the development process utilizes the Model Based Design (MBD) engineering methodology. The method is applied and associated with control systems and design of embedded software as a common framework for communication and integration with the traditional development cycle known as the V-model. The four steps of the model are: plant modeling, controller synthesizing, plant-controller simulations and integration by deploying the controller [5].

The general structure for the method applied to the thesis is as follows:

- **Modelling and Simulation:**
  Model and simulate the system in MATLAB and Simulink commonly known as Model In the Loop (MIL) simulation.
- **Automatic Code Generation:**
  Generate the controller code by building the Simulink-models to C++ code in order to run the code on the hardware.
- **Rapid Prototyping:**
  A quick way of manufacturing the physical parts needed with Computer Aided Design (CAD) in combination with 3D printing or additive manufacturing.
- **Hardware In the Loop Simulation:**
  Build the auto-generated C++ code on the actual hardware and simulate with the controllers.
- **Integration and Test:**
  Integrate the models and controllers in the car to validate the actual behaviour with the expected results from the simulations.

The results from the simulations and the tests on the actual hardware is then compared and analysed before vehicle implementation. Some variation is expected due to communication delays between the interacting systems and limitations in hardware.

1.4 Delimitations

A main delimitation of this thesis is that the development do not follow any specific safety standard. For future iterations, this needs to be addressed.

All aspects of implementation that is carried out through the project relates to Volvos Scalable Product Architecture (SPA) platform. This being available for testing through Volvo Cars. The steering gear in the SPA platform is made by an external supplier, hence its source code is unknown.

The main goal is to develop a compact steering device that can be used as a backup in autonomous cars when manual steering is required. The outcome of the project should not be expected as a complete single-solution alternative to the traditional steering wheel.

Due to general time constraints, this thesis will only focus on a smaller steering wheel design to be able to generate feedback torque with a small geared direct current (DC) motor. Joysticks and other types of steering input devices requiring different methods of providing the driver with feedback torque will not be investigated.

Similarly, the control strategies used in this project were limited to less complex ones in order to reduce development time and decrease the risks of project delays.

1.5 Related research

As mentioned, SbW is a topic of increasing interest for major car manufacturers that are investing time and money into research and development. Previous work include modelling of the relevant systems [6] and investigating different approaches on obtaining feedback torque.

The work includes differences between open and closed-loop methods for force-feedback. Closed-loop possibilities like torque and position control proved to be more effective in terms of inertia compensating and reference tracking compared to open-loop control which lacked equal tracking performance due to shortcomings related to force feedback motor impedance [7] [8].

Although the majority of work conducted in the area focuses on SbW systems still utilising the traditional steering wheel with the normal size and location, studies concerning human-vehicle interaction investigating different approaches to steering input has also been conducted.

Some early examples of alternative steering input devices include the modified Saab 9000 as a part of the Pan-European research project Prometheus [1] and the Mercedes-Benz F200 Concept car. Both examples were early concepts of the joystick as primary steering input device in a complete Steer-by-Wire system. Because of the limited range of motion of the joystick compared to the traditional steering wheel, it was difficult to obtain good steering attributes with the joystick for both high and low speed maneuvers [9].

Investigation into joystick steering for handicapped drivers using wheelchairs has been performed, where the joystick is used for both steering and acceleration/deceleration [10]. The work mentioned was improved for high speed driving by introducing different variable sensitivity methods to cope with various driving situations. The limited inclination range of the joystick could therefore be better optimized for both parking and high speed driving [11].

In order to simulate the system, models for the components are needed. Several studies have been conducted regarding the modelling of steering gears for cars. The models derived in this thesis are based on the work of Steve Fankem, Thomas Weiskircher and Steffen Mülles conference paper demonstrating the steering rack modelling of a car [12].

The torques acting on a steering gear are well documented at Volvo. However, as

they assume the usage of a large steering wheel, the project turned instead to the work of Kristoffer Tagesson, Bengt Jacobson and Leo Laine for their investigation regarding how feedback torque should change for different steering wheel sizes [13].

Safety in automotive applications is imperative and heavily restricted. In order to concretise the potential safety hazards of automotive systems they can be evaluated using different standardized methods [3]. Some of these are:

- **ISO26262 - Road vehicles – Functional safety** - International standard that is used to derive a ASIL rating of a system and guide development [14]
- **HAZOP** - Hazard and Operability Study [15]
- **FMEA** - Functional Failure Modes and Effects Analysis [16]

Methods like these could be used in the project to evaluate the safety of the device and state possible improvements in case of further development.

One proposed method of improving system safety is an electro-mechanical dual-redundancy design of implementing an extra angle sensor, actuator and controller [17]. Other examples include a SbW system with selective braking used as backup steering [18] and a system utilising a duo duplex structure for failure detection and redundancy management [19].

1.5.1 Objective metrics and test scenarios for steering systems

ISO - the International Organization for Standardization has a number of standards for test procedures of passenger vehicles to establish repeatable and discriminatory test results. The standards *ISO 13674-1: Weave Test* and *ISO 13674-2: On-center handling* are procedures for steering systems in closely controlled test environments, meaning that they are not applicable to real driving conditions.

These standards evaluate the dynamical behaviour of the vehicle in terms of on-centre handling, usually at relatively high speeds. On-centre handling is a description of "steering feel" in relation to vehicle precision at high speeds, which is not included in the thesis scope.

In order to test the performance of the implemented SbW system, where angle tracking between steering wheel and steering rack for varying frequencies in low speeds is the thing of interest, other tests need to be performed.

1.5.2 Previous work

The force feedback delivered to the driver was investigated in an earlier thesis project conducted at Volvo Cars by Martin Johannesson and Henrik Lillberg. The thesis was a comparison between open-loop angular, closed-loop angular and torque feedback controllers [20].

Their finding showed that for a SbW system, torque feedback controller are superior with regards to reference tracking of a desired transfer function. The area

of operation of the systems they investigated were frequencies below or equal to 5 Hz. The study also showed that open-loop controllers had worse performance due to the dynamics of the motor.

Torque sensors however are generally regarded as expensive hardware, and in a effort to reduce complexity of the steering device, this thesis project will strive to generate the steering torque from models or calculating it from the current consumption of motors together with its torque constant.

1.6 Outline

The chapters of the thesis are introduced and explained below:
Chapter 1: Introduction

- This chapter includes background, problem description, approach, related research and thesis goal.

Chapter 2: System description

- Explanations and fundamental theory about the concepts and systems mentioned in the report.

Chapter 3: System control strategy

- The method of implementing different control strategies and general explanations.

Chapter 4: Implementation

- The process of implementing the designed models and regulators as a complete functional system in a vehicle implementation

Chapter 5: System modelling

- The process/method of modelling the entire system to be able to simulate and obtain results.

Chapter 6: Results

- Presentation of results from controller implementation, comparison between model versus hardware implementation and a summary of a user study performed.

Chapter 7: Discussion

- Discussion of why the models differs from reality and analysis of the different stages of development.

Chapter 8: Summary

- Summary of the work carried out in the thesis and suggestions of further development and areas with room for improvement.

2

System Description

The following chapter aims to introduce the reader to the components used in the various project sub-systems and clarify terms and principles related to the area.

2.1 Steer-by-Wire

In a conventional system where the steering wheel is mechanically connected to the road, as shown in Figure 2.1, it is still possible to steer the vehicle in case of electric power assisted steering (EPAS) failure. This is due to the fact that modern power steering only functions as an assisting feature.

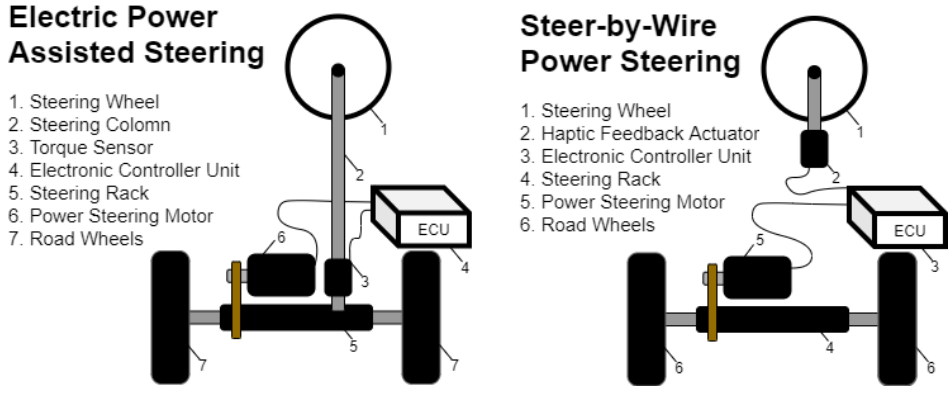

Figure 2.1: *Comparison between conventional and SbW systems*

SbW systems usually consist of the following components:

- Human Interface Device, traditionally a steering wheel.
- Sensors, for instance torque or angle.
- Haptic feedback actuator, usually a servo motor.
- Steering rack actuator, usually the integrated power steering motor which translates rotational action to linear.

With a full SbW system, the steering column is replaced by actuators and control systems to steer the car, a system overview is shown in Figure 2.1 with general components for both types of steering systems. Since steering is one of the most safety critical systems of a car, redundancy and fail-safe procedures needs to be implemented in other ways.

An intermediate SbW system retains the steering column in case of an electrical failure. The ECU will detect an error and mechanically connect the steering column with a clutch [3]. The main advantages of SbW is lost with an intermediate system since the complete mechanical connection to the road wheels is still required.

In a SbW system, when the driver applies torque to the steering wheel it is registered by the car as a control signal and an output is sent to the steering rack actuator. In some scenarios, a mathematical model of the vehicle can be used to calculate the corresponding torque that the driver should feel for the specific scenario, which is then generated by means of the haptic force feedback motor. The simpler approach is to use the actual forces acting on the steering wheels, which also feeds disturbances from the road to the driver.

2.1.1 Electronic control unit (ECU)

With increased complexity regarding sensors and actuators in passenger cars, the ECU is a type of embedded system that controls one or more actuators to achieve a specific function. The control unit receives electrical input signals from all the relevant sensors and outputs electrical control signals to all the actuators used to perform the specific tasks.

The electronic control unit used in EPAS systems is called electric power steering control unit (PSCU). Driver steering input signals in terms of torque and speed of the steering wheel with absolute precision are sent to the PSCU, which calculates required steering assistance from the servo motor based on position, rotational speed and direction of the steering wheel. The control unit also verifies sensor signals and can detect faulty components [21].

Modern vehicles today typically contains more than 70 ECUs that controls different safety-critical systems. The most relevant bus standard used for communication between controller units, sensor and actuators for the project is called Controller Area Network (CAN) and will be described in the following section.

2.1.2 Controller area network (CAN)

The Controller Area Network (CAN) was developed in 1985 by Bosch as a method to have robust communication between the growing number of electronic subsystems in cars. The system is today fully adopted in the automotive and other electro-mechanical industries. It is used as a standard for transmitting data between different ECUs in modern vehicles and is since 1993 a international standard, *ISO11898* [22].

The structure of CAN messages include several bits that are used for transmission of information and error checking. These are however not relevant for many users and the actual information that is sent and received in CAN messages consists of two main functional components, the identifier and the data. The identifier tells the protocol what the signal is, while the data contains the information of the signal.

The identifier is traditionally made from 11 bits, there are however newer expansions of the protocol that offers up to 29 bits [23].

In order to obtain and send data to and from the steering device, CAN will have an integral role in the thesis project. The communication will be integrated with offline controllers deployed in HIL prototyping platforms, such as dSPACE Autobox or a Vector VN-modules [24] [25].

All the systems mentioned above are for instance subject to ISO26262, a unified safety standard for vehicle electrical and electronic safety-related systems. The increasing complexity of vehicle electronic systems lead to the introduction of the risk-based safety standard intended for passenger cars with a focus on safety critical components during all phases of the product life cycle [26].

2.2 Force feedback in Steer-by-Wire systems

When the mechanical steering column is removed, new solutions for force feedback torque generation is required. The EPAS motor commonly used in steering gears is a brushless synchronous motor (BSM) which is also often used as force feedback motor in SbW applications. This thesis will investigate the possible benefits and implications of using a smaller DC motor instead.

The general principle of an electric motor is converting electrical energy to mechanical energy. Electric motors are categorized by type of supply current; alternating current (AC) or direct current (DC). The DC type motors are then typically divided into two groups based on the type of construction and commutation. The first is a brushed type, where the rotor has coil windings and the stator is either a permanent magnet or an electromagnet [23].

2.2.1 Brushless DC motor

Brushless DC motors (BLDC), are DC motors that instead of using commutator brushes to reverse the electric polarity, uses electronically controlled energizing of the windings to generate torque. They have in recent years increased in popularity due to advances in commutator circuits.

This thesis will utilize BLDC motors as feedback due to overall good power to size ratio. The construction of the brushless type of DC motors is reversed compared to brushed types, the rotor is a permanent magnet and the stator has the coil windings.

This type of motors have three windings, with each winding being capable of reversing polarity, the motor goes through six different voltage phases in each revolution. Due to the energizing of the coils only depending on where in these six steps the motor is, the resolution of any sensor only has to be 6 pulses/rev to be able to control the commutation. This is why most BLDC motors comes with three internal hall-sensors used to control commutation. The Hall-sensors are capable of detecting positive or negative magnetic fields and hence provide sufficient resolution [23].

Four quadrant (4-Q) BLDC motor control

BLDC motor control is split into different quadrants dependant on direction of rotation and torque. The most simple controller acting in quadrant one and three can only apply torque in the same direction as rotation. Controllers also acting in quadrant two and four can provide torque in the opposite direction of rotation and are called 4-Q controllers. This means that the motor can act as a brake when the torque is applied in the opposite direction of the rotation. This is a requirement in force feedback implementations in order to supply the driver with feedback torque in the opposite direction of the steering input rotation [27].

2.3 Sensors

Sensors primarily used in SbW systems are torque and angle sensor which will be briefly explained in this section.

2.3.1 Angle sensor

Angular displacement can be measured by digital outputs from optical encoders which can be divided into two categories: incremental encoders and absolute encoders.

Incremental encoder

The encoder consists of a rotating disc with slots combined with a light source and sensor. When the disc rotates the light sensor outputs a pulse proportional

to the rotated angle. Usually the disc consists of three tracks, two are the same spacing with a small offset in order to determine the direction of rotation. The resulting signal from this can be seen in Figure 2.2, where A and B are separate sensors that are offset. The final track only consists of one slot and is used to locate a type of home position [23].

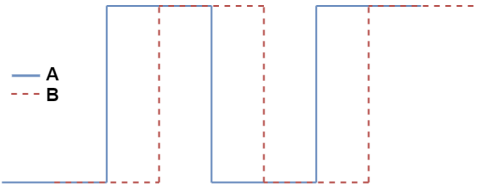

Figure 2.2: *Typical encoder pulse train*

Absolute encoder

The basic principle of the absolute encoder is an extension of the incremental where the tracks forms a specific binary number for each angular segment. The total number of bits in the binary number will be the same as the number of tracks which in turn describes the resolution of the encoder. If 10 tracks are used, the resolution of the encoder will be $\frac{360}{2^{10}} = 0.35°$ [23].

2.3.2 Torque sensor

When the driver applies torque on the steering wheel, the torsion bar is twisted. Optical encoders on each end of the torsion bar measure the angular difference and combined with the torsion bar stiffness, the torque can be calculated together with steering wheel angle [21].

Some torque sensors used in the electric power steering system utilize the magnetoresistive principle, where rotation of a magnet in relation to the sensor creates a change in magnetic field. The magnetoresistive element changes resistance when the field direction changes, which in turn can be interpreted as measured torque [28].

3

System control strategies

There are different ways of modelling and controlling the system depending on which of several control strategies that is chosen for the task. The three most suitable strategies for this project and its time frame is explained in the following Chapter.

3.1 Open-loop speed control

In the approach seen in Figure 3.1, there is no angle feedback between the steering wheel or the steering rack. This means that only scaling factors are present. The current that is consumed by the force feedback motor in order to regulate its speed is scaled with the motors torque constant and sent to the steering gear as applied torque working in the steering wheel. This is then perceived by the EPAS as input to move the steering gear, the resulting speed of the steering gear is then sent to the force feedback motor as the speed request. This is the simplest implementation since there is no need for a feedback controller or the position of the steering device, removing the need of precise movement sensors and decreasing the overall system cost.

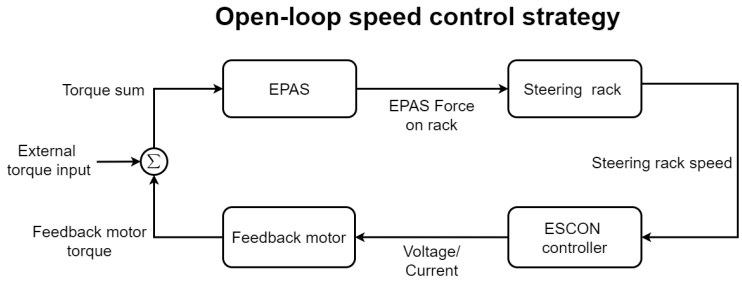

Figure 3.1: *Open-loop controller*

Open loop control in this manner does however allow for drifting, a phenomena that appears when an outside stimulant surpasses the amplification properties. When this happens, the position of the rack may move even though the steering wheel is stationary. Something that may manifest itself for instance when a large force is acting continuously on the wheels of the car while the driver maintains constant angle input, the system may then move unintentionally.

The open-loop controller feeds the force feedback motor with a voltage proportional to the speed. When a load is applied to the motor, the speed will decrease. With a speed sensor and known speed/voltage constant some controllers utilise an adaptive compensation that adjust for the difference, giving a type of feedback called Rx compensation.

3.2 Closed-loop angle control

In the approach seen in Figure 3.2, the angle of the SbW hand-wheel is required as it uses two position controllers, both of which work towards minimizing the angular error between the hand-wheel and steering rack.

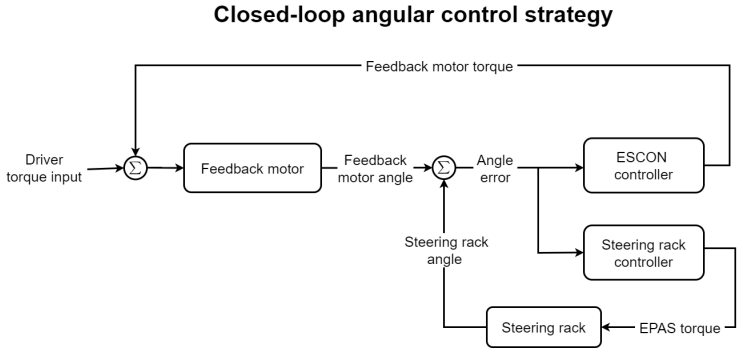

Figure 3.2: *Closed-loop angle controller*

These two controllers can be divided into one that turns the wheels of the car and one controller that supplies force feedback to the driver. One controller outputs emulated torque to the servo steering on the gear while the other controller outputs torque request sent to the force feedback controller. The feedback of the actual angle of the steering device offers greater robustness against the problem with drifting. In both this method and the open-loop speed control method, any movement of the steering rack affects the torque felt by the driver. This means that the force feedback is transferred from to road to the driver without any model estimations.

3.3 Reference generated feedback

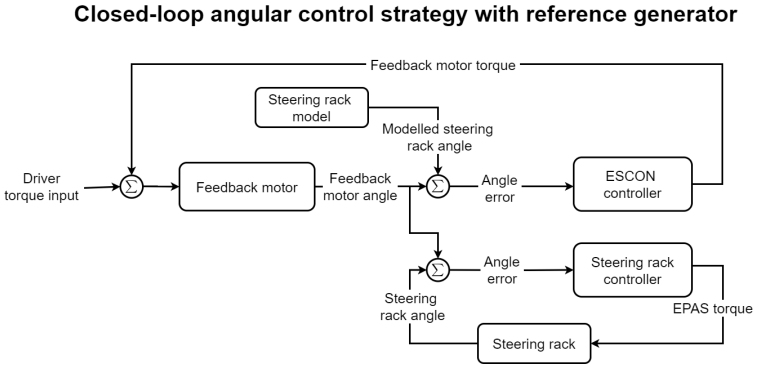

Figure 3.3: *Closed-loop angle controller with reference generator*

The approach seen in Figure 3.3 shares many similarities with *closed-loop angle control*, in the ways that the angle from the SbW hand-wheel is used to control the power steering. The force feedback to the driver is, however, in this case computed using a reference generator. A reference generator is a mathematical model that calculates the forces acting on the wheels of the car based on active vehicle parameters such as velocity, steering angle and mass. From these calculated forces, the resulting torque that the driver would feel can be derived based on the different gearing ratios between the SbW steering wheel and steering gear.

This is an implementation that allows the force feedback to only contain driving essential information and not road disturbances such as potholes. By doing this, an improved user experience can be achieved as the input will feel smoother. As this controller requires a good model of the vehicle in order to deliver an intuitive experience it is only introduced here for further iterations of the project.

4

Implementation

The following chapter describes the overall hardware implementation in test rig and vehicle.

4.1 Hardware implementation

The interaction and subsystems are shown in Figure 4.1, where solid boxes represent hardware and dashed boxes represent software used to configure hardware.

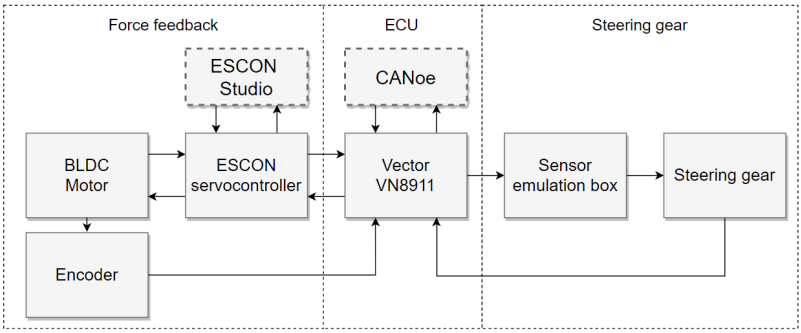

Figure 4.1: *Steer-by-wire implementation overview*

The two boxes on the left hand side in Figure 4.1 represents the steering device with force feedback motor controller while the two boxes on the right hand side represents the rack control with the sensor emulation box. A VN8911 is used

to house the controllers and support communication as a stand-alone prototype ECU.

The system was designed so that transition from test rig to car only involved switching one single connection, the torque sensor mounted on the steering column is disconnected from the steering gear ECU and a bypass connector from the emergency breaker is instead connected to the steering gear from the sensor emulator. Apart from the computer monitoring the system and providing a Vector license, all systems require no more than 12 V from the car.

4.1.1 Steering input versions

Rapid prototyping using CAD and 3D-printing was performed to find a suitable steering input design. The 3D-printed steering device is made in plastic was supplemented with an adapter part, manufactured in metal for the motor axle in order to distribute the torque input on a greater surface area. This reduces the stress on the plastic steering wheel and facilitates testing of different wheel designs.

The final designs are shown in Figure 4.2, 4.3 and 4.4. Two utilises Brodie knobs to facilitate multiple revolution steering input without the need of releasing the wheel. In the third design, this is achieved by static "hooks" in the design.

Figure 4.2: *Steering device design 1 with small (65 mm) diameter and a retractable Brodie knob*

Figure 4.3: *Steering device design 2 with larger diameter (80 mm) and permanent Brodie knob*

Figure 4.4: *Steering device design 3 with medium (70 mm) diameter and hooks*

4.1.2 Force feedback motor

The BLDC motor used as force feedback motor in the thesis is a Maxon EC-max 30, rated at 12V and 60W. A planetary gearbox with the ratio 33:1 is mounted on the motor shaft in order to obtain requested speed/torque characteristics. The backlash of the planetary gearbox creates a dead-zone of 0.7 degrees. The motor is controlled with a Maxon ESCON 50/5 4-Q servo controller, which is compatible with the ESCON Studio software.

The servo controller has a number of analog and digital I/O ports used for communication with the network interface. The controller allows different modes of operation for the BLDC motor which includes open-loop speed control, closed-loop speed control and current control. The overall schematic of the controllers are shown in Figure 4.5. In the project, the current controller strategy is implemented.

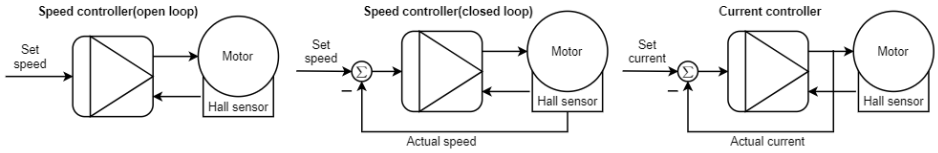

Figure 4.5: *Description of the different BLDC control strategies*

In addition to the embedded hall sensors, the BLDC motor could be delivered with an axle mounted encoder for an additional cost. Unfortunaly this was not done and the encoder proved to be essential for closed-loop control of the BLDC motor due to resolution limitations concerning the hall sensors. Since the encoder could not be retrofitted to the motor, an alternative solution was created.

Instead, the optical encoder of a mouse scroll wheel is used in combination with a 3D-printed disc shown in Figure 4.6. The rotary encoder consists of two infrared photo detectors, one infrared LED, combined with the 30 slots on the disc resulting in a total resolution of 120 pulses per revolution of the BLDC motor shaft. With the ratio of the gearbox, the steering device resolution is 3960 pulses per revolution which is enough to enable closed-loop position control of the motor.

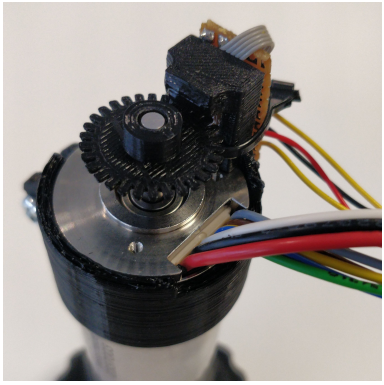

Figure 4.6: *Rotary encoder used on the motor shaft*

4.1.3 Network Interface - Prototype ECU

The network interface is a modular Vector VN8911 with added support for multiple CAN channels and I/O ports. The development and testing software CANoe from Vector is used to control and monitor the system. Network nodes in CANoe can either run compiled Simulink models or CAPL-scripts, which is a procedural programming language similar to C, developed by Vector Informatik. Controllers used in this project are compiled into such nodes and run stand-alone on the Vector hardware acting as a prototype ECU.

In the scenario of open-loop control, the VN8911 receives an analog signal from the ESCON proportional to the averaged current consumed by the BLDC motor and in the scenario of closed-loop position control, the digital signals from the infrared photodioides are directly connected to the VN8911. The actual pinion position and speed is sent as a CAN message from the steering gear to the VN8911 where it is translated into a digital PWM signal for the ESCON controller to control the force feedback speed or torque of the motor.

Resolution conversion

The analog output from the BLDC controller has a 12-bit resolution that spans a voltage interval of -4 to +4 Volt; referenced to a common GND. Unfortunately the analog input of the VN8911 IOpiggy has a 12-bit resolution that spans a voltage interval of 0 to 36 Volt.

That means that in order to read the negative sensor values, the signal from the BLDC-controller needs to be offset by +4 Volt as well as being scaled up with a factor of $\frac{Range_2}{Range_1} = \frac{36V}{8V} = 4.5$ in order to use the full resolution of both systems.

Using the circuit shown in Figure 4.7, the [-4, +4] output is converted into a [0,+12] V analog input to the Vector device.

As mentioned, the ideal solution would scale to 36 V, the full range of the analog input. However, since the majority of subsystems are supplied with 12 V in the car, this is the most practical solution since it eliminates the need of a step-up converter. Unfortunately, this means that the signal resolution is reduced to $\frac{12}{36} \cdot 2^{12} \approx 1365$ bits of resolution. This resolution is however sufficient for the system.

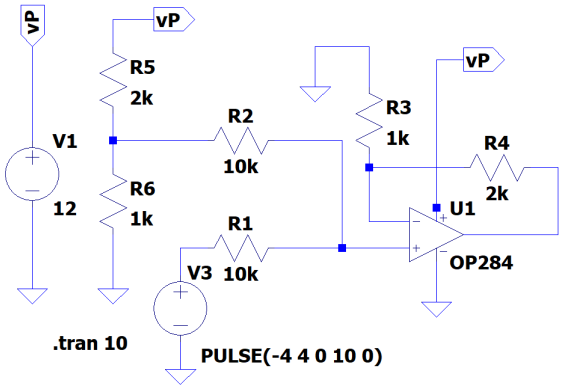

Figure 4.7: *Operational amplifier circuit with voltage dividers simulated in LTspice*

4.1.4 Steering gear

The steering gear used in the project is found in the SPA platform from Volvo. It has an internal ECU, or PSCU, that controls the EPAS motor. For this ECU to function it needs to be connected to the chassis CAN-network as well as having torque sensor input from the traditional steering wheel. The implementation of the steering device aims to be non-destructive, meaning that the steering gear of the car does not need to be in any way modified.

The EPAS motor in the test rig shown in Figure 4.8 is limited to 16 amperes due to the power supply used.

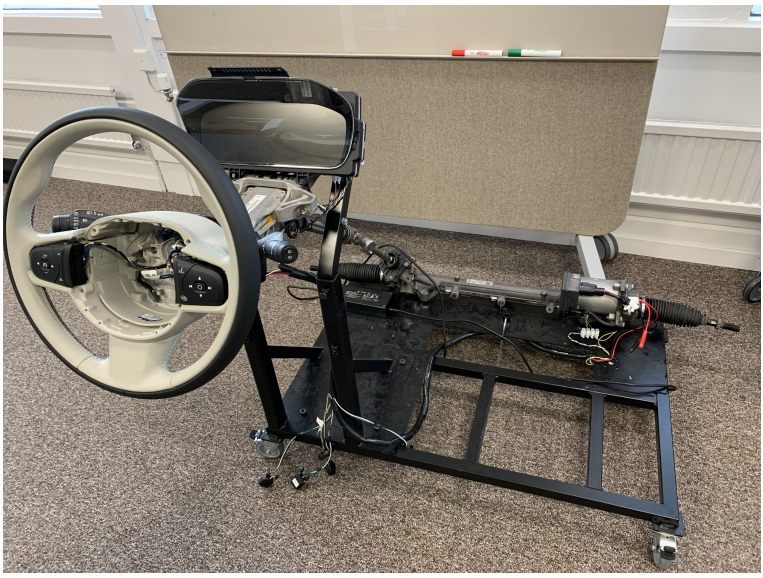

Figure 4.8: *SPA test rig used during the implementation*

4.1.5 Sensor emulator

The communication between the network interface and the steering gear is performed by a sensor emulation box from H2 Mechatronic Systems GmbH. The emulation box replicates the same signal usually sent from the traditional steering wheel torque sensor to the ECU of the EPAS motor. The emulation box communicates with the network interface device via CAN. Two messages are required for operation; mode and required torque.

The CAN message is interpreted by the emulation box and directly sent to the PSCU which controls the EPAS motor. However, the resolution of the CAN signal was limited to 0.0390625 Nm per step, which can reduce resolution for control of the gear to some extent. Since no modification of the EPAS ECU is done, return to center is still active in the background.

4.2 System safety

An easy and cost effective way of implementing system safety in the development phase is the utilization of an emergency stop which disconnects the torque sensor emulator. Instead, the torque sensor measuring steering wheel torque is connected to the steering gear ECU in order to have full control of the vehicle with assistance in case of system failure.

Testing of the emergency switch on a standalone steering gear showed that going uninterrupted from sensor emulator to original torque sensor induced aggressive unpredictable movement of the steering rack. Hence, using the emergency switch to go between the two sensors could instead lead to a new hazardous scenario. The solution became to use a manual switch in combination with the emergency stop to introduce a dead zone where no sensor is engaged. The different signal flow scenarios can be seen in Figure 4.9.

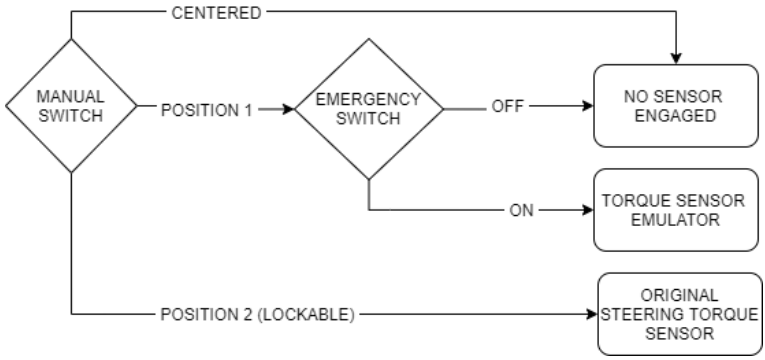

Figure 4.9: *Torque sensor safety flowchart*

This is only a viable alternative for prototyping on vehicles with the mechanical connection between steering wheel and road wheels still present. Vehicles with no mechanical connection require additional safety functions in terms of redundancy.

As for the software and controller implementation, there are many simple features that can be added to further increase the safety and stability of the overall system. The first one being to add "on/off"-switches for any embedded controller that needs to be manually turned on after start-up. This forces the driver to actively engage the prototype system. These switches can also automatically be controlled in case of abnormal behaviour.

In the case of the closed-loop controllers, they both are working towards minimizing the angular error between the angle of the steering device and the steering rack.

A safety implementation for this scenario that also was implemented was that the controllers were automatically switched off if the angular error between the

steering wheel and the steering rack was greater than 1 rad. This gate also serves to ensure that the controllers initially cannot be turned on if the error between the sub-systems is too great, which removes the possibility of aggressive behaviour on start-up.

When starting the system, the 1 rad dead-zone also worked to ensure that the controllers did not do aggressive maneuvers since the hand-wheel always initiates to centered position. Meaning that if the car was parked with a large angle on the wheels, this could lead to a large angular error being sent to the controllers when the car was started. A problem that became more prominent when the system moved from test rig to vehicle, where even an error-skip of 1 rad could lead to unwanted behaviour. This was solved by modifying the controllers to only start when the angle of the road wheels corresponded to the angle of the steering device.

Since the motor was fitted with both optical encoders and hall sensors to measure the movement of the force feedback motor shaft, they are used to cross-reference respective speeds to each other. This redundancy will greatly decrease the encoder errors ability to endanger the driver.

Another redundancy can be found in the duality of the encoders photo-diodes. Since there always is a predetermined pattern to the pulse train, as seen in Figure 2.2, any deviation from this pattern means that the signal has been corrupted. Small deviations can be tolerated due to the high resolution of the encoder, as mentioned in Section 4.1.2 a complete revolution of the steering device results in 3960 pulses. However, a large number of missed steps during a short duration induces abnormal behaviour and can be used to disable the influence of the Steer-by-Wire system.

4.3 Vehicle implementation

Figure 4.10 shows the 3D-printed steering device holder located in the centre console. The holder is mounted with a type of interference fit in order to not damage the interior of the vehicle. Figure 4.11 shows the general driving position and Figure 4.12 shows the VN8911 and sensor emulation box located on the armrest between the rear seats.

Different steering devices with the shapes and sizes mentioned in Section 4.1.1 could all be tested without any major modifications since the different steering device design prototypes are easily removed by a single screw on the top. The ESCON controller, VN8911 network device and the sensor emulation box all require 12 volts from the auxiliary power outlet in the car. A laptop is also needed since the Vector CANoe license is bound to the computer.

Controller parameters can be tuned in real time during vehicle tests with CANoe system variables mapped to the compiled Simulink model running on the VN8911.

Figure 4.10: *Steering device placement in the centre console*

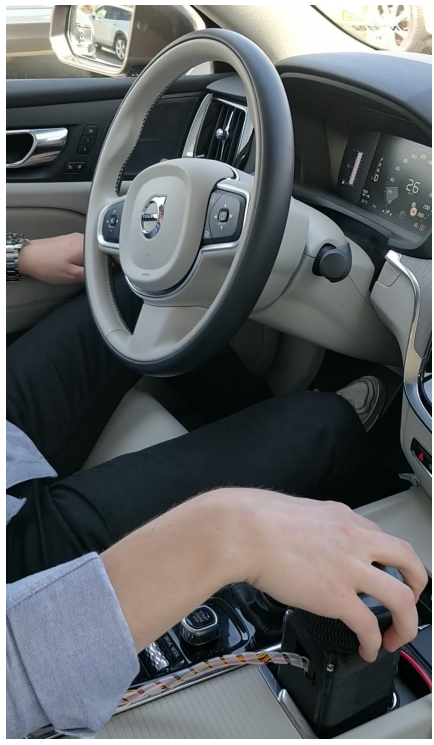

Figure 4.11: *In-car use of device*

Figure 4.12: *VN8911 and sensor emulation box placement on the arm-rest between the rear seats*

5
System modelling

The following chapter describes the process of modelling the system. Simulated models will be compared to the actual system in terms of performance in the final stages of the report. Actual parameter values used in the simulations will not be revealed due to secrecy.

The modelling process is split into physical modelling and identification. The physical modelling involves breaking down the system into subsystems with known properties. Identification is used to fit the unknown model properties to the system properties by observations [29].

5.1 Steering device and force feedback motor

The component brakedown shown in Figure 5.1 of the steering device, force feedback motor and the planetary gearbox is modelled with the parameters in Table 5.1.

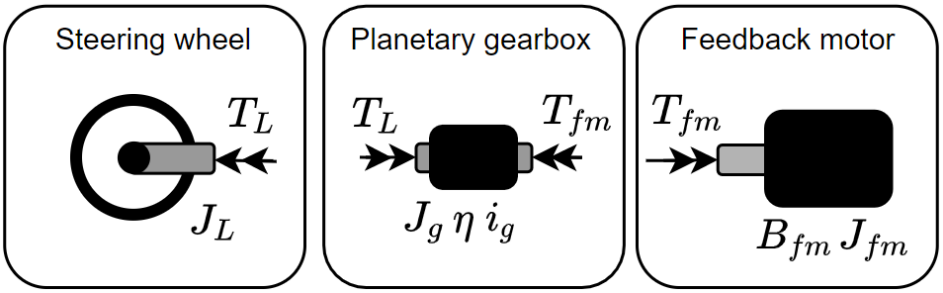

Figure 5.1: *Component brakedown of the steering device with force feedback motor and planetary gearbox*

Table 5.1: *Steering device and force feedback motor parameters*

Notation	Parameter	Unit
T_{fm}	Force feedback motor torque	Nm
T_L	Load torque	Nm
i_{gb}	Planetary gear ratio	-
J_{fm}	Force feedback motor moment of inertia	kgm^2
J_g	Planetary gearbox moment of inertia	kgm^2
J_L	Load moment of inertia	kgm^2
η	Planetary gearbox efficiency	-
B_{fm}	Force feedback motor viscous friction coefficient	Nm s/rad
θ_{fm}	Force feedback motor angle	rad
$\dot{\theta}_{fm}$	Force feedback motor angular velocity	rad/s
$\ddot{\theta}_{fm}$	Force feedback motor angular acceleration	rad/s^2

5.1.1 Force feedback motor and planetary gear

The steering system is modelled as

$$T_{fm} = \frac{T_L}{i_{gb}\eta} + (J_{fm} + J_g + \frac{J_L}{i_{gb}^2\eta})\,\ddot{\theta}_{fm} + B_{fm}\,\dot{\theta}_{fm} \tag{5.1}$$

Where the force feedback motor torque T_{fm} is the sum of the load torque T_L and the contributions from inertia and friction coefficients. The planetary gearbox ratio is denoted by i_{gb} and is used with the gearbox efficiency η. Force feedback motor angular acceleration $\ddot{\theta}_{fm}$ is linked by Euler's second law of motion with the sum of the acting inertias, force feedback motor inertia J_{fm}, gearbox inertia J_g and load inertia J_L, which is the approximated inertia of the steering input device. Force feedback motor angular velocity $\dot{\theta}_{fm}$ is used together with the viscous friction coefficient of the force feedback motor B_{fm}.

The transfer function from torque to angular velocity for the open-loop speed

control system using Laplace transform is

$$\theta_{fm}\, s = \frac{1}{(J_{fm} + J_g + \frac{J_L}{i_{gb}^2 \eta})\, s + B_{fm}} (T_{fm} - \frac{T_L}{i_{gb}\, \eta}) \tag{5.2}$$

The transfer function from input torque to force feedback motor angle for the closed-loop current control system using Laplace transform is

$$\theta_{fm} = \frac{1}{(J_{fm} + J_g + \frac{J_L}{i_{gb}^2 \eta})\, s^2 + B_{fm}\, s} (T_{fm} - \frac{T_L}{i_{gb}\, \eta}) \tag{5.3}$$

Model validation for the open-loop speed control system

In order to validate the force feedback system described in Section 4.1.2, a speed request in terms of a PWM signal is sent to the ESCON servocontroller, which is then converted to a proper 3-phase DC voltage and current for the BLDC motor. As this is done by the embedded controller in the ESCON, it is treated as a black-box and replaced with a PID in the model. The corresponding speed signal in RPM described in Table 5.2 is tested in a Simulink model in order to compare the current response. The speed in the model is also reduced by the ratio of the planetary gearbox.

Table 5.2: *PWM signal in relation to BLDC speed in RPM for the different validation tests*

	PWM [%]	Speed [RPM]
Test 1:	30	1995
Test 2:	50	4986
Test 3:	80	6983

Figure 5.2 through 5.4 shows the simulated current in relation to the actual current obtained from hardware tests. The current is calculated using the known torque constant of the motor. Ignoring the noise of the actual system and some variation in overshoots, the model is a good representation of the actual system in terms of current consumption for different speed requests.

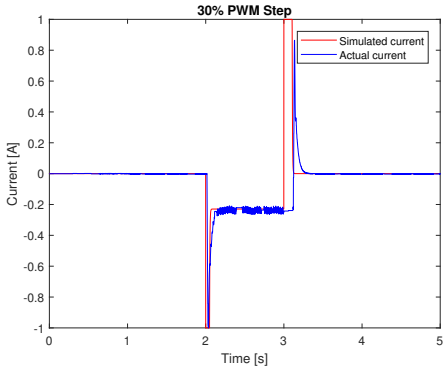

Figure 5.2: *Force feedback system validation for a PWM step of 30%*

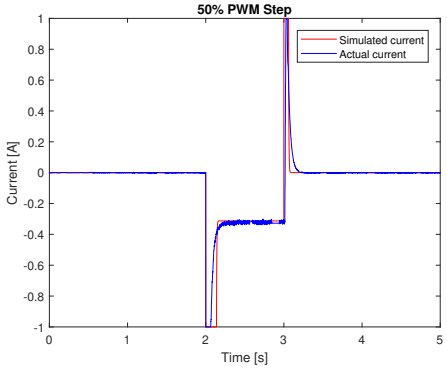

Figure 5.3: *Force feedback system validation for a PWM step of 50%*

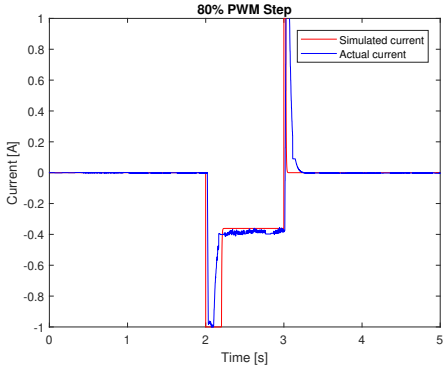

Figure 5.4: *Force feedback system validation for a PWM step of 80%*

Model validation for the closed-loop angle control system

The force feedback motor for the closed-loop angle control system is validated by performing a ramp in angle request and comparing the feedback motor angle for the model and the actual system. Figure 5.5 and 5.6 the validation for two different ramp angle requests. The delay seen in the plots are mainly caused by delays in communication between the computer and the network device. The result was rather unpredictable due to friction in the planetary gearbox and communication issues, which explains the stationary error.

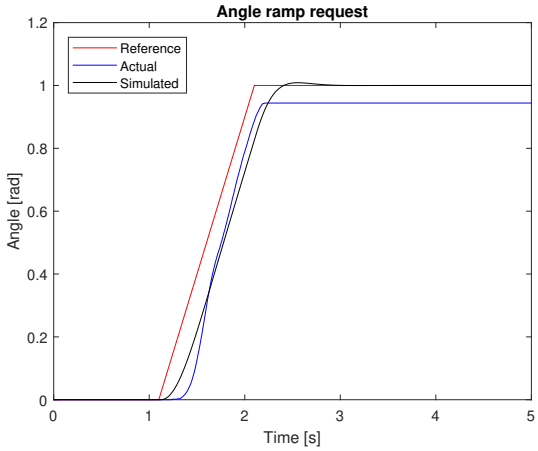

Figure 5.5: *Model validation for ramp signal with slope of 1 from 0 to 1*

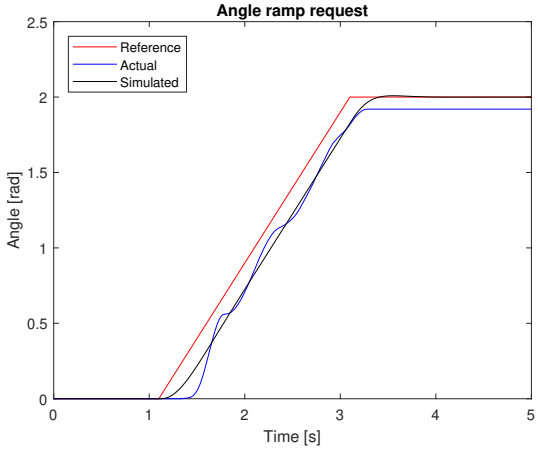

Figure 5.6: *Model validation for ramp signal with slope of 1 from 0 to 2*

5.1.2 Driver model

The driver is modelled as a PID-controller, where the proportional gain corresponds to the stiffness of the driver arm and the derivative gain corresponds to the damping of the driver arm. Assuming that the driver is able to converge actual steering wheel angle to requested angle, an integral gain is also implemented.

The requested steering wheel angle is compared to the actual steering wheel angle, which is translated to a torque signal for the force feedback motor system.

5.1.3 Variable steering ratio and feedback

As mentioned in Chapter 1, one advantage with a SbW system compared to a traditional steering wheel assembly, is the ability to actively change the angle ratio between steering wheel angle and road wheel angle based on vehicle speed. An other alternative is to actively change feedback torque at different speeds to stiffen the steering wheel at higher speeds and reducing at lower speeds. This is realized by multiplying the feedback motor request with a variable gain based on vehicle speed. The final implemented system in the car will utilize a tuned combination of these two solutions.

Traditional rack and pinion steering systems may have variable ratios by changing the distance between gear teeth on different parts of the rack. This may for example lead to a less sensitive behaviour at high speed with the steering wheel close to centre, something that also can be implemented in a SbW system.

5.2 Steering rack and EPAS motor

The steering rack model is a transfer function derived using force equilibrium equations from the three main components shown in Figure 4.8: steering wheel with column, power steering motor and steering rack. Description of component breakdown can be seen in Figure 5.7 and parameters and units can be found in Table 5.3. The external forces that acts on the steering rack, F_{ext}, are included in the equations. However, as the model comparison is performed on a stand-alone steering gear they are generally assumed to be equal to zero during the project.

Table 5.3: *Steering rack and EPAS motor parameters*

Notation	Parameter	Unit
θ_m	EPAS motor angle	rad
T_m	EPAS motor torque	Nm
F_m	EPAS motor force on rack	N
K_m	EPAS motor friction	Nm
J_m	EPAS motor moment of inertia	$\mathrm{kg\,m^2}$
θ_s	Steering column angle	rad
T_s	Steering column torque	Nm
F_s	Steering column force on rack	N
K_s	Steering column friction	Nm
J_s	Steering column moment of inertia	$\mathrm{kg\,m^2}$
x_r	Rack position	m
m	Rack mass	kg
F_B	EPAS boost curve based force on rack	N
i_p	Pinion gear ratio	$\mathrm{m^{-1}}$
i_g	Ball and screw-gear ratio	$\mathrm{m^{-1}}$
G	Transmission ratio	–

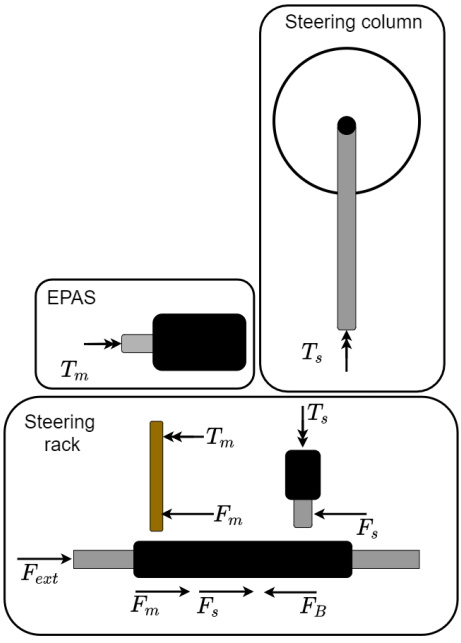

Figure 5.7: *Steering rack and EPAS components*

Steering column

The force equilibrium of the steering column and steering wheel is given by:

$$J_s \ddot{\theta}_s + K_s \dot{\theta}_s = T_s \tag{5.4}$$

The column and steering wheel are assumed to share parameters for inertia, J_s and friction k_s. Inertia is based on the angular acceleration of the steering column, $\ddot{\theta}_s$ where as the friction is based on the angular velocity, $\dot{\theta}_s$.

T_s is the torque present at the pinion from the steering gear. Since the rotational movement of the steering column is converted into a linear motion through the means of a rack and pinion gear with a ratio i_p, the motion of the rack and pinion x_r are linked by $x_r\, i_p = \theta_s$. This in turn gives the correlation between rack force and pinion torque as:

$$F_s \frac{1}{i_p} = T_s \tag{5.5}$$

These conversions of motion and energy added to equation (5.4) results in an equation showing the linear force acting on the steering rack from the friction and inertia of the steering column:

$$J_s\, {i_p}^2\, \ddot{x}_r + K_s\, {i_p}^2\, \dot{x}_r = F_s \tag{5.6}$$

EPAS motor

The force equilibrium of the power steering motor wheel is given by:

$$J_m \ddot{\theta}_m + K_m \dot{\theta}_m = T_m \tag{5.7}$$

Where inertia is given by the inertia constant J_m and angular acceleration of the EPAS motor $\ddot{\theta}_m$. The friction is given by the friction constant K_s and the angular velocity of the motor $\dot{\theta}_m$. Since the rotational movement of the EPAS motor, θ_r is converted into a linear force F_m through the means of ball and screw-gear with a ratio i_g and a belt transmission with ratio G, the motion of the motor and the rack are linked by $x_r\, i_g\, G = \theta_m$. This in turn gives the correlation between rack force and motor torque from inertia and friction as:

$$F_m \frac{1}{i_g\, G} = T_m \tag{5.8}$$

In a similar manor to the modified rack and pinion relation (5.6), the inertia and friction of the EPAS motor acting on the rack is given by:

$$J_m \, {i_g}^2 \, G^2 \, \ddot{x}_r + K_m {i_g}^2 \, G^2 \, \dot{x}_r = F_m \tag{5.9}$$

Steering rack

The force equilibrium of the steering rack is:

$$m \, \ddot{x}_r = F_B - F_s - F_m \tag{5.10}$$

Where F_B is the applied force on the rack from the power steering motor based on a mapped boost-curve.

By substituting the linear contributions of the steering column and EPAS motor from Equation (5.10) the equation for the entire rack is obtained as:

$$m \, \ddot{x}_r = F_B - (J_s \, {i_p}^2 \, \ddot{x}_r + K_s \, {i_p}^2 \, \dot{x}_r) - (J_m \, {i_g}^2 \, G^2 \, \ddot{x}_r + K_m \, {i_g}^2 \, G^2 \, \dot{x}_r) \tag{5.11}$$

When the derived states are substituted by the Laplace constant s, F_B can be expressed as:

$$\begin{aligned} F_B &= m \, s^2 \, x_r + J_s \, {i_p}^2 \, s^2 \, x_r + K_s \, {i_p}^2 \, s \, x_r + J_m \, {i_g}^2 \, G^2 \, s^2 \, x_r + K_m \, {i_g}^2 \, G^2 \, s \, x_r \\ &= (m \, s^2 + J_s \, {i_p}^2 \, s^2 + K_s \, {i_p}^2 \, s + J_m \, {i_g}^2 \, G^2 \, s^2 + K_m \, {i_g}^2 \, G^2 \, s) \, x_r \\ &= (m \, s^2 + J_s \, {i_p}^2 \, s^2 + K_s \, {i_p}^2 \, s + J_m \, {i_g}^2 \, G^2 \, s^2 + K_m \, {i_g}^2 \, G^2 \, s) \, \frac{1}{i_p} \, \theta_s \end{aligned} \tag{5.12}$$

Which inverted results in:

$$\theta_s = \frac{i_p}{(m \, s^2 + J_s \, {i_p}^2 \, s^2 + K_s \, {i_p}^2 \, s + J_m \, {i_g}^2 \, G^2 \, s^2 + K_m \, {i_g}^2 \, G^2 \, s)} \, F_B \tag{5.13}$$

Which is the transfer function from force applied on the rack by the EPAS boost curve to pinion angle of the steering rack, henceforth known as G_{rack}.

Model implementation and validation

From the equations described above, a Simulink subsystem corresponding to the EPAS steering gear was developed. It includes the transfer function of the steering rack, the boost curve that corresponds to force applied on the rack from the EPAS, dead-zone for torques lower than 0.3 Nm as well as saturation of torque sent to the rack.

The need of both the dead-zone and the saturation was based on experience from working with the steering rack, showing that the steering gear was hard to control

with torque request lower than 0.3 Nm due to internal friction and that the power supply cuts out when performing fast transitions if there was no limit on torque. The implementation of these attributes can be seen in Figure 5.8.

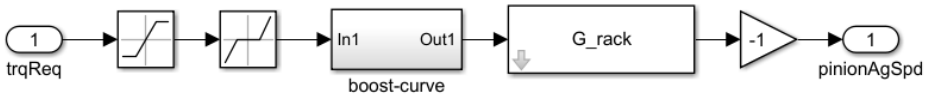

Figure 5.8: *Simulink sub-system of steering gear*

Unfortunately the values of the mapping for the boost-curve are covered by confidentiality from Volvo Cars and can not be disclosed.

In order to validate the model, a script that conducted a number of open-loop torque steps to the steering gear was developed. The script collects pinion angle response of all steps and saves them to a .MAT-file from which a mean step response for a certain amount of torque applied could be calculated. The steps were conducted by sending pulses of 0.8 Nm and 1 Nm for 0.5 seconds using a Simulink model that in combination with a Vector VN8911 sent the request through the sensor emulator. These measurements were used to gray-box tune the model since the unmodified step responses of the model had similar behaviour but too large values compared to the actual steering gear.

The Vector logged and stored the movement of the steering gear and sent it to the MATLAB workspace. Since the steps had many small variations in stationary values and rise time, the model validation was performed with aspect to the average of all steps. The validations can be seen in Figure 5.9 and 5.10 where it can be observed that the model behaviour is close to that of an average step in the test rig.

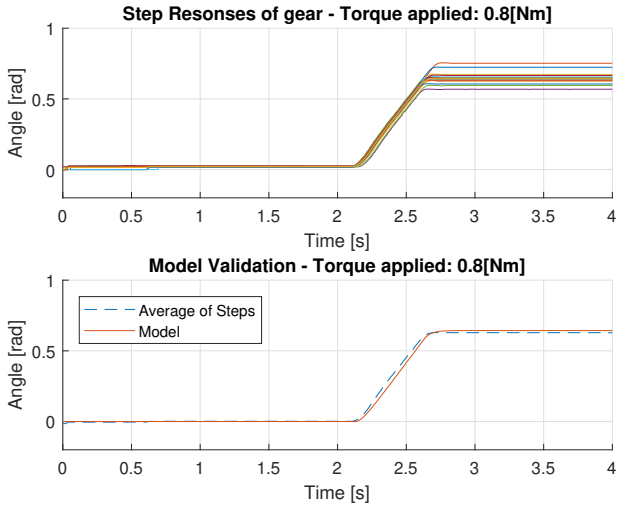

Figure 5.9: *Step responses and model validation for steps of 0.8 Nm.*

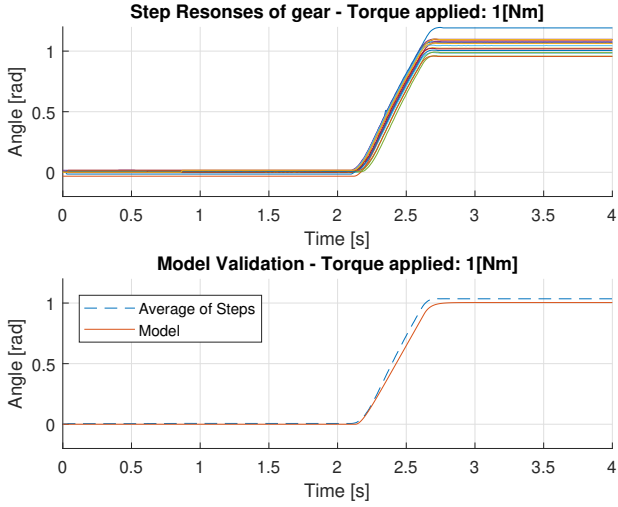

Figure 5.10: *Step responses and model validation for steps of 1 Nm.*

6
Results

The following chapter presents the results of the tests performed on the implementations. The main focus was to evaluate the differences between the measured and the modelled system. A user study was also performed as the system became drive-able well before the end of the project.

6.1 Viability of controller design

The project started with the aim of investigating an open-loop speed controller since this was the least complex of the methods proposed in Chapter 3 in terms of simplifying the transition from model to implementation.

This was also the primary strategy since the lack of encoder in combination with hall sensor feedback proved to be insufficient for precise control of the BLDC motor at low speeds.

Following extensive tuning and filtering with a moving average filter, the controller performed well and smooth with no load present on the rack. However, when a load was applied to counteract the movement of the steering gear, the BLDC had a tendency to drift since the speed controller in the ESCON was unable to accurately counteract the speed applied by the driver on the steering device.

The reduced resolution of the analog speed signal between the ESCON and VN8911 discussed in Section 4.1.3 may also have contributed to the poor performance of the open-loop speed controller.

The drifting could to some extent be circumvented by using variable temperature resistance compensation available through the ESCON controller, giving a stiff enough response to driver torque that the motor would not skip commutation

angles. Unfortunately, the required stiffness of the SbW device led to oscillations and unpleasant aggressive behaviour when performing fast maneuvers on the test rig.

This unwanted behaviour led to the action of developing an in-house optical encoder as mentioned in Chapter 4. The encoder enabled the project to utilise the position of the SbW device in a closed-loop angular controller. In this configuration, there were instead two position controllers that could be individually tuned from a traditional PID structure. This also increased signal robustness compared to the open-loop controller which used average current consumption sent from the ESCON to the Vector as an analog signal. The signal had to be converted multiple times before being acted on as well as the problem of analog signals being prone to electromagnetic interference (EMI). The optical encoder instead used in the closed-loop strategy sends pulses directly to the Vector and the embedded controllers.

From the lessons learned during the implementation, it was clear that the open-loop controller was not a viable option with the hardware available and it was abandoned for closed-loop angular control. Since the scope of thesis included the physical vehicle implementation, the reference generated feedback option was abandoned due to general time constraints regarding developing a fully functional vehicle model.

6.2 Closed-loop angle control system - Chirp signal response

The test involves sending a chirp signal with varying frequency from 0.2 Hz to 3 Hz as requested angle. The rack and wheels should be able to follow the requested angle without any major and unpredictable oscillations and delays.

Figure 6.1 and 6.2 shows the result of the modelled system compared to the test rig in terms of following a reference angle for the steering. With no access to a steering robot, the reference angle had to be implemented as the requested angle sent to the controller from the hand wheel.

The loss of reference tracking at higher frequencies can partially be explained by the current limit of the test rig power supply. The torque sensor emulation box had to be limited by implementing a saturation at 1.33 Nm. Otherwise, the power supply would cut power to the EPAS motor when the torque request was too large.

Overall, the models developed, follow the real components to a sufficient degree and could in the future be used to test and tune further controller designs.

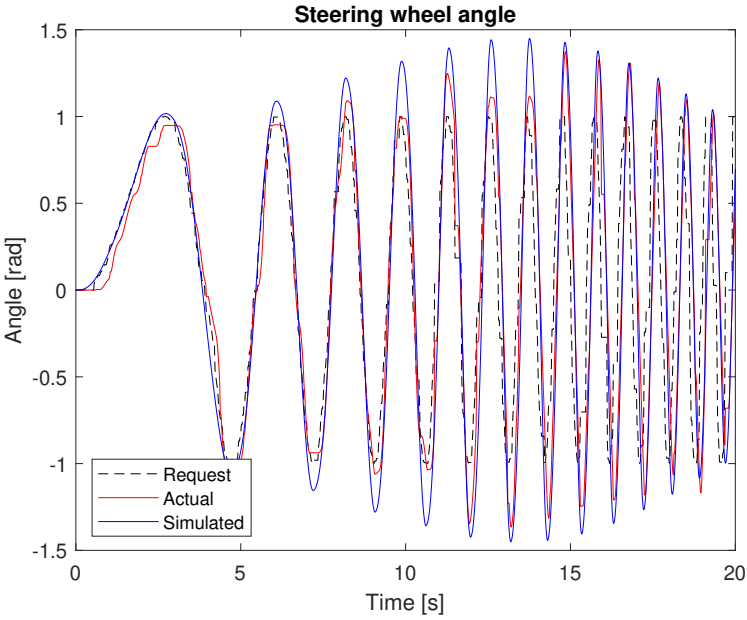

Figure 6.1: *Modelled versus simulated steering device angles*

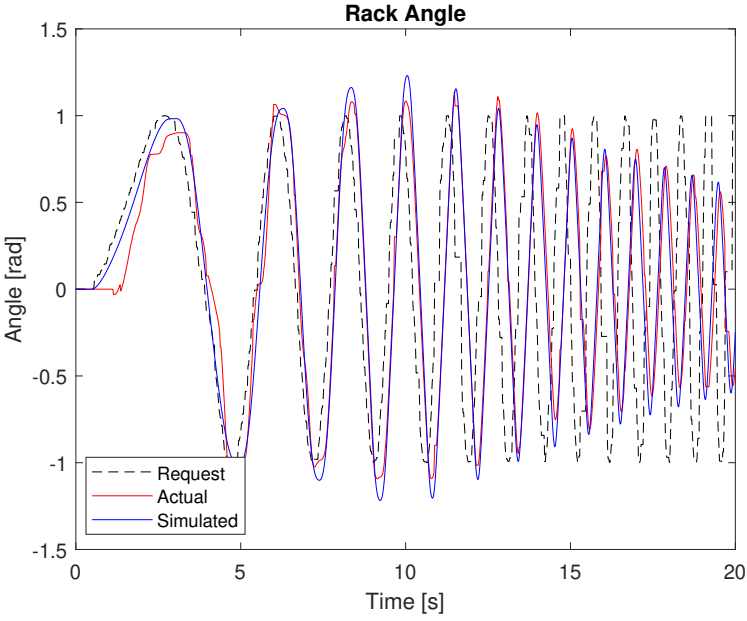

Figure 6.2: *Modelled versus simulated rack pinion angles*

6.3 Vehicle test results

The vehicle with the implemented closed-loop angle control system was tested and tuned on a test track at the Volvo Cars Torslanda plant. The angular results from both the hand steering device and the steering gears pinion position can be seen in Figure 6.3. Due to the lack of a steering robot, vehicle testing and tuning was performed manually. Initially, the PID controllers tuned in the test rig were underdimensioned due external loads acting on the vehicle. This was solved by some further tuning in vehicle, where only tuning for good reference tracking was not the top priority. Instead, drive-ability was more related to how responsive the system was without experiencing delays.

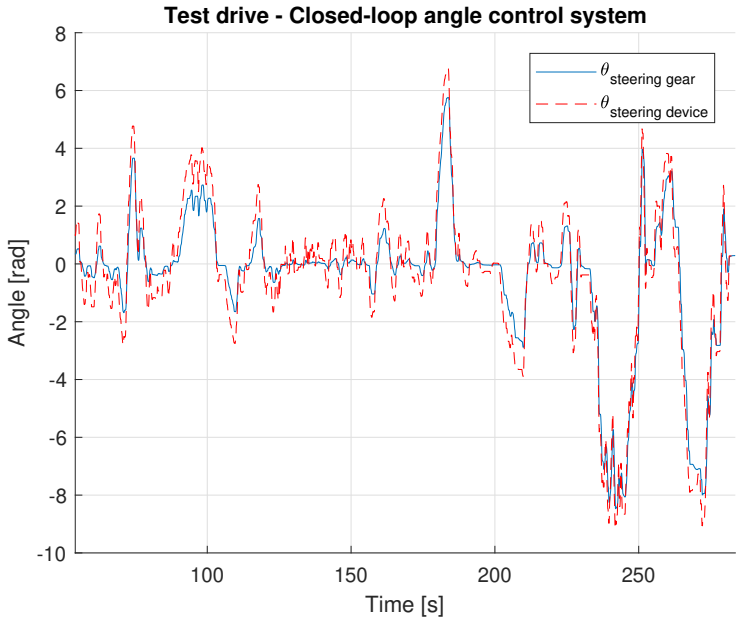

Figure 6.3: *Angular results from test drive on Volvo test track*

It can be seen that the spring behaviour of the proportional parts of the closed-loop controllers naturally filter out much of the noise-like behaviour induced by small jerks on the SbW device whilst maintaining the overall characteristics when maneuvering.

The stationary error whilst driving was not noticeable, the responsiveness and lack of system delays was far more important when tuning in regards to drive-ability and steering feel. After tuning, the final controllers were two PD-controllers. Also, a ratio of 2.3 between the hand-wheel and the traditional steering was added to facilitate large steering inputs considering the relatively limited range of motion of the wrist.

The final implementation utilized a variable ratio based on vehicle speed, where the ratio was increased to 3 at speeds below 15 km/h. This solution improved low speed maneuvers whilst maintaining overall good steering characteristics at medium to high speed maneuvers.

6.4 User study

As mentioned in Section 1.2, a user study was performed where 39 people at Volvo were allowed to drive the modified Volvo S60 at the Torslanda grounds. These people included members of development areas close to the project, blue-collar workers and senior management at Volvo Cars. Out of this group, twenty five people chose to answered the user study. Figure 6.4 through 6.7 presents the results from the user study for each question.

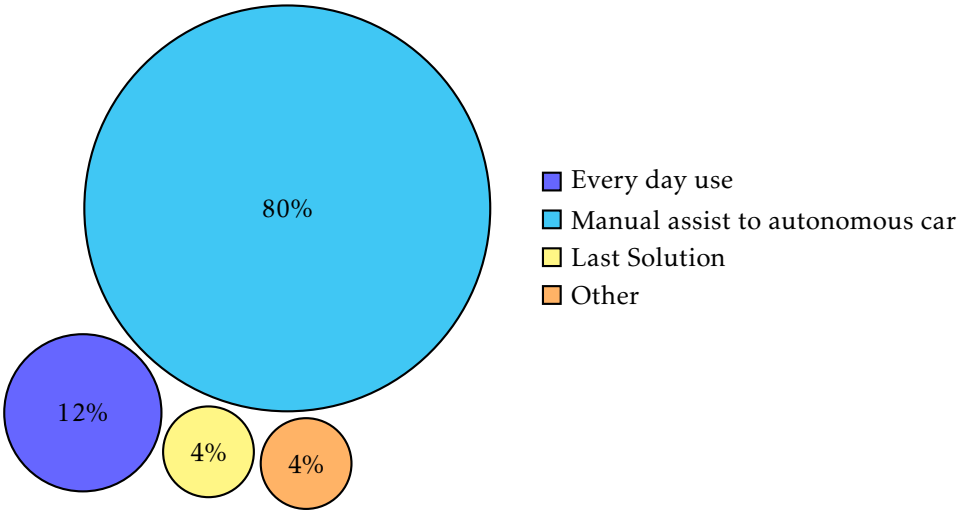

Note: The answer *Never* had zero responses and were excluded

Figure 6.4: *In what scenario do you see yourself driving a car with an alternative steering device?*

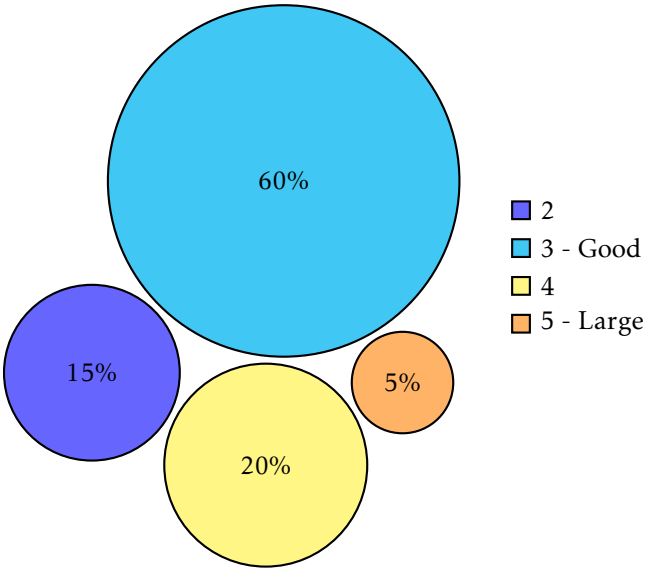

Note: The answer *1 - Small* had zero responses and were excluded

Figure 6.5: *What did you think about the size of the steering device?*
Answers are on scale from *(1 - Small)* to *(5 - Large)*

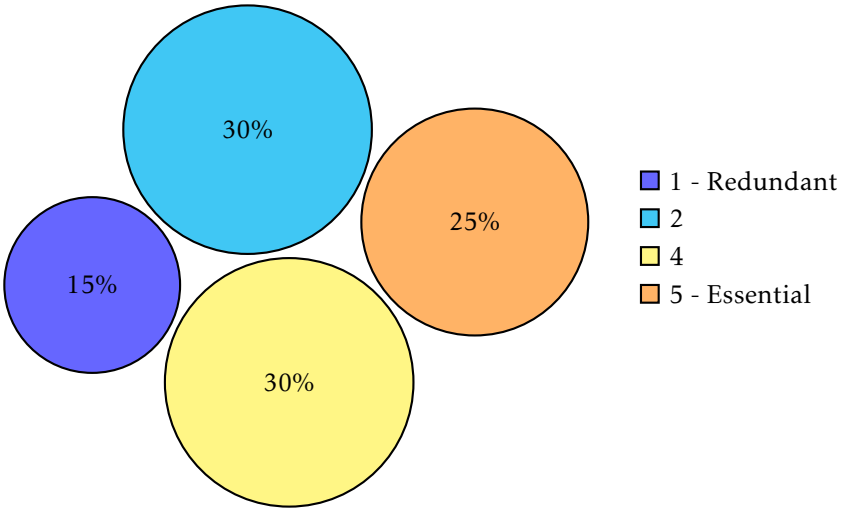

Note: The answer *3 - Indifferent* had zero responses and were excluded

Figure 6.6: *To what extent did you feel that a Brodie-knob was necessary?*
Answers are on scale from *(1 - Redundant)* to *(5 - Essential)*

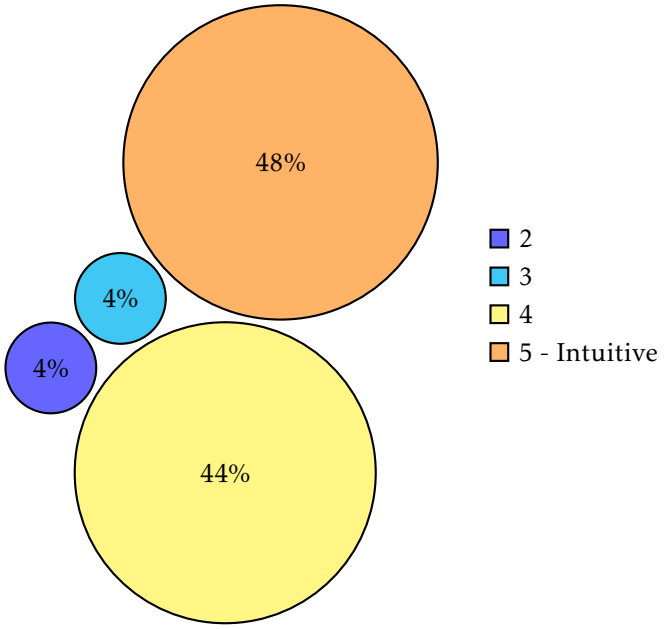

Note: The answer *1 - Non-intuitive* had zero responses and were excluded

Figure 6.7: *What did you think about the driver experience?*
Answers are on scale from *(1 - Non-intuitive)* to *(5 - Intuitive)*

As shown in Figures 6.4 and 6.7 above, the overall feedback from the test drivers were positive. The majority of drivers thought that the system could be a manual assistant to the steering in autonomous cars with an intuitive driver experience. The size of the steering device (80mm) was found to be good as seen in Figure 6.5. However, the necessity of a Brodie knob was questioned by a lot of drivers as seen in Figure 6.6.

It was a clear opinion of several drivers that the action of obtaining a new grip was unpleasant and problematic, one driver implied that the grooves seen in design 1 was helpful. Several drivers preferred using the Brodie knob due to these reasons, though its usage often received comments on lowering the overall steering feel.

Multiple drivers raised the question of having a variable output depending on speed. The need of which became prevalent when performing 90 degree turns at low speeds, for instance when turning onto a main road from a side road. Some drivers pointed out that the movement of the ordinary steering wheel was distracting and that the experience was enhanced when trying to ignore it, they suggested that the device should for future generations be tested in a car without steering wheel. Alternatively, implementing the system in a right-hand drive car with access to brake and gas pedals on the left side.

While many drivers pointed out that the dead zone induced by the planetary gearbox was noticeable when first interacting with the device, no one felt that it

was problematic whilst driving.

It was a popular opinion between the drivers that the device was "surprisingly controllable" and that the learning period was short even for new drivers. A impression shared by the project members, all-though biased.

There were mixed feeling regarding the placement of the steering device with some individuals requesting a lower position whilst some responded negatively to the suggestion. This issue was mainly caused by the lack of freedom to mount the system in ways that would damage the vehicle interior.

7
Discussion

The following chapter describes and discusses conclusions based on the results of the simulations and implementations.

7.1 Discussion and analysis

Using hardware with the essential sensors, it is possible to steer a car with an alternative input steering device which requires less space compared to the traditional steering wheel whilst still remaining force feedback from the road. A brushless DC motor is a good alternative since it offers high power in a compact package and there is a large variety of motors and gears to choose from. The complexity of the motor controller leads to many unknown functions when modelling since the motor has to have an external commutator controller, which is unknown to the user. It is possible to gain some insight through the data-sheets and software of the part. However, things like conversion, resolution and transport delays remain unknown in the modelling part of the project.

Throughout the project, it has been clear that the irregular behaviour of static friction in the different transmissions as well as the transitions between movement and stationary is the greatest source of deviation between models and reality. This is clear in the case of the planetary gear of the driver force feedback motor. This friction is also a part of the decision to use the smoother movement of the steering racks angular velocity for the derivative parts in both the steering rack position controllers and steering device force feedback controllers.

7.1.1 Model implementation

Both model in the loop simulations developed, showed that parameters in the models needed adjustment to match their behaviours with the corresponding validation test of the individual components. This type of *Gray-box modeling* proved necessary for the controllers as well, since their behaviour when using the parameters originally tuned with the models differed from simulated response when applied on the steering rack test rig.

The overall conclusion was that models not adjusted to actual measurements gave insufficient insight to the real world behaviour of the system. The best method of approach for such a rapid prototyping project proved to be the usage of a steering gear test rig as this allowed for the development of robust communication and tuning of controllers that could have been potentially hazardous to develop in a car.

Since the rig had no external loads and a limiting power supply, the controllers were initially underdimensioned when transitioning to vehicle testing. The overall structure, however, proved viable and the only modification required to drive the car was to increase the proportional gain of the steering gear controller. Theoretically, it would be possible to utilise the models in order to find more suitable controller parameters in terms of reference following. However, this was not a project priority since the goal of the controllers was not only objective, but also subjective as driving feel.

A large source of deviation from model to reality is the inevitable fact that the source code of the of component of the steering system was not available to the project. Unknown components were treated as black-boxes and estimated based on measurements.

For example, as mentioned in Section 1.4, the steering gear of the Volvo SPA platform is manufactured by an external supplier with undisclosed dynamics of its underlying features and controllers. The complexity of the full system model would also be so intricate that it would have to be cross-referenced with real world measurements.

Since the steering input substitutes the input from the driver torque sensor, EPAS features like return to center also remain active in the background. This proved useful as a way of simulating road forces on the steering gear when working in HIL-mode but was also a feature that would be difficult to implement in the MIL of a project of this scope.

7.1.2 Vehicle implementation

Whilst transitioning from steering rig to car, it became clear that fast reference following did not correspond to good driving ability and intuitive behaviour. Most noticeable was when performing fast maneuvers, which was possible due to the small size of the steering device. Following extensive tuning performed in car, the steering device eventually became predictable and smooth. A Volvo S60 with

the system was driven extensively at the Volvo Torslanda grounds, where the device performed well in situations such as parking, low-velocity handling and medium velocity city handling.

Whilst driving, the angular error did not need to be close to zero for intuitive driving as the driver is used to some flex from the torsion bar found in ordinary steering. There is, however, a clear difference in driver experience between spring related errors and backlash related errors. The flexing that appeared due to the proportional gain of the controllers improved the drive, while the dead-zone from the gear-box in the force feedback motor induced lower quality of control when performing fine adjustments around the centre position.

The force feedback motor proved to be overdimensioned when using it in a car. Maximum permissible power of the motor was $60W$, having a nominal current of $4.72A$. When supplying the motor with $12V$ and $1A$, the steering device was strong enough to stop the driver input. If severe torque were applied by the driver to the steering device the motor could struggle to maintain a stationary position. However, to inform the driver of an end stop the torque was suitable.

There is also a safety aspect as to why not having a over-dimensioned force feedback motor is preferable. The force feedback is not a driving critical system and as long as the encoder with steering rack controller is functional, the driver is able to steer the vehicle. If the force feedback motor instead would be able to overpower the driver it can exclude the driver from vehicle control.

To get a pleasant range of motion, a ratio between the SbW device and the steering rack was induced. The final ratio after tuning was around $x2.3$, meaning one rotation of the steering device resulted in two full rotations of the steering gears pinion angle which correlates to the traditional steering wheel angle.

Whilst performing small inputs on the SbW device, for instance tuning adjustments for lane following, an unpleasantly large amount of input had to be delivered by the driver. To compensate for this, the amplification of the controllers in car was increased which solved the problem of fine movements while allowing the driver to make excessively aggressive maneuvers as the steering device now was more powerful than drivers are used to. Since the control strategy was satisfactory for low frequency responses, a rate controller that dampened aggressiveness was added.

The rate controller multiplies the angular velocity of the steering rack with a small number in order to get a controller input smaller than 1. This input is then squared in order to get an input designed to react fast for angular speeds higher than desired. The output of the rate controller limits the torque sent to the sensor emulator in order to limit the aggressiveness of large errors whilst still allowing high power fine tuning.

7.1.3 The implementation of variable ratios and gains

Different methods and strategies were tested to implement the variable ratios and gains described in Section 5.1.3 based on the desire to obtain different steering characteristics during various driving situations.

The first implementation was based on an increased ratio with increased distance to the centre of the rack. In theory, this would mean stable vehicle handling with small movements of the steering device whilst at the same time obtaining the necessary ratio to perform tasks like parking and low speed maneuvers without unreasonable large steering inputs.

However, this type of variable ratio caused some issues with the intuitive driving experience. When performing steering inputs from end lock to end lock, the different ratios on the various parts of the rack created a rather unpredictable steering behaviour with jerky movements. Therefore, the strategy was abandoned and focus was instead shifted to a variable ratio strategy based on vehicle speed.

With the limited test time available in vehicle, the strategy was difficult to implement in an intuitive manner. When changing the angle ratios at different vehicle velocities, gaps in angle control were introduced. The different ratios also lead to overall poor regulator behavior and performance for all types of driving situations.

Instead of changing the angle ratio, another solution was to implement an increasing force feedback based on vehicle velocity which proved to be effective in terms of maintaining a relatively high angle ratio at higher velocities. With a stiffer steering device at higher speeds, the driving feel was more smooth and stable.

8
Summary

The following chapter concludes and summarises the work done in the thesis. Possible future work in the area is also presented.

8.1 Summary and conclusions

A complete solution as an alternative steering input device was modelled in simulation and implemented in a Volvo S60. The completed system achieved all the requested attributes and functions described below:

- Provide a solution for manual steering in autonomous cars
- Minimal space-usage and no permanent modification to the vehicle
- Should be able to handle parking and low speed maneuvers safely

The steering device design was limited relatively early to a small hand wheel as this shared some resemblance to the usual steering interface that drivers use, while allowing for a shorter time span needed to find suitable parts.

Feedback torque is delivered to the driver by means of a brushless DC motor with an optical encoder. Interaction and computation between the steering device, controllers and the steering gear of the car is performed using an Vector VN8911 prototyping platform.

Communication between different components of the system is performed using CAN networks, digital I/O interfaces and serial communication to connect the VN8911 and computer.

Comparing the model to the actual test rig proved to be difficult due to unknown parameters, various communication delays and unknown embedded code in some components.

Initially, developing the system, the controllers were tuned for good reference following and the ability to handle quick responses. Something that proved futile when transitioning from test rig to car as the behaviour translated to poor usability. The smaller steering device allowed for movement which lead vehicle behaviour perceived by the driver as jerky and aggressive.

Instead, the controllers were tuned for user exposure, which allowed for a highly intuitive driving experience.

To relay the experiences of test drivers to future development projects, a user study was performed with Volvo Car employees. Data was collected with regards to steering device design, usability and personal opinions.

To summarise the general opinions of the test drivers, the device offered high maneuverability and the learning period was overall short. The vast majority was under the perception that they could use the steering device as an manual option in an autonomous car. Some drivers reported that they could potentially use it as an every-day alternative, while some regarded it as a final solution in case of autonomous break down.

Overall, we are quite pleased that the device became good enough for vehicle implementation despite the narrow time-frame a master thesis offers.

8.2 Future work

Possible future improvements of the system includes further analysis regarding system safety and overall hardware improvements. For example, if the force feedback motor would malfunction, the driver would not be able to obtain force feedback and would simply rely on the angle signal from the encoder to steer the car with the current setup.

By implementing two direct drive feedback motors connected in series with individual certified sensors and controllers, the issue would partly be resolved. Combined with smarter controllers, the need for a planetary gearbox would disappear, meaning that the overall size of the device would basically be the same whilst eliminating the discussed dead-zone affecting the drive-ability.

With the implementation of a purpose-made ECU for the task as well, communication errors and delays would improve due to the decrease in the total number of subsystems communicating with each other. The issue concerning Vector CANoe license would also disappear together with the system requirement of using a computer in the vehicle.

Investigation regarding more complex control strategies compared to the chosen PD-control strategy in combination with some way of implementing vehicle

speed based ratios and gains is also an interesting area of improvement for future iterations of the project.

Bibliography

[1] Carl Legelius. Minns du saaben utan ratt - ersatt av joystick? *Svenska Dagbladet*, 3(19), 2019.

[2] Paul Yih. Steer-by-wire: Implications for vehicle handling and safety, 2005. URL `http://www-cdr.stanford.edu/dynamic/bywire/dissertation.pdf`. Visited 28-January-2020.

[3] C Becker, J Brewer, D Arthur, and F Attioui. Functional safety assessment of a generic steer-by-wire steering system with active steering and four-wheel steering features. *Washington, DC: National Highway Traffic Safety Administration*, 2018.

[4] Kristof Polmans. Torque vectoring as redundant steering for automated driving. In Peter Pfeffer, editor, *5th International Munich Chassis Symposium 2014*, pages 163–177. Springer Vieweg, 2014.

[5] W Chaaban, M Schwarz, B Batchulunn, H Sheng, and J Börcsök. A hil test bench for verification and validation purposes of model-based developed applications using simulink and opc da technology. *ELECO 2011 7th International Conference on Electrical and Electronics Engineering*, 2011.

[6] Albin Gröndahl. Functional modelling and simulation of an electric power assisted steering. *Master's thesis in Automotive Engineering*, Chalmers University of Technology, 2018.

[7] Tushar Chugh. Haptic feedback control methods for steering systems. *Thesis for the degree of Licentiate – Department of Mechanics and Maritime Sciences: 2019:05*, Chalmers tekniska högskola, 2019.

[8] Tushar Chugh, Fredrik Bruzelius, Matthijs Klomp, and Barys Shyrokau. Design of haptic feedback control for steer-by-wire. *2018 21st International Conference on Intelligent Transportation Systems (ITSC)*, 2018.

[9] Jonathan M. Gitlin. Why you'll never drive your car with a joystick. *Ars Technica*, 6(25), 2014.

[10] Masayoshi Wada and Fuijo Kameda. A joystick type car drive interface for wheelchair users. *RO-MAN 2009 - The 18th IEEE International Symposium on Robot and Human Interactive Communication*, 2009.

[11] Masayoshi Wada, Fuijo Kameda, and Yukimichi Saito. A joystick steering control system with variable sensitivity for stable high speed driving. *IECON 2013 - 39th Annual Conference of the IEEE Industrial Electronics Society*, 2013.

[12] Steve Fankem, Thomas Weiskircher, and Steffen Müller. Model-based rack force estimation for electric power steering. *IFAC Proceedings Volumes*, 47th(3), 2014.

[13] Kristoffer Tagesson, Bengt Jacobson, and Leo Laine. The influence of steering wheel size when tuning power assistance. *International Journal of Heavy Vehicle Systems*, 21(4), 2014.

[14] International Organization for Standardization. Iso 26262-3, 2017. URL `https://www.iso.org/standard/68383.html`. Visited 13-February-2020.

[15] SEK Svensk Elstandard. Ss-en 61882, 2020. URL `https://www.sis.se/produkter/foretagsorganisation/foretagsorganisation-och-foretagsledning-ledningssystem/produktion-produktionsstyrning/ssen61882/`. Visited 13-February-2020.

[16] Six-sigma. Fmea - failure mode and effect analysis, 2020. URL `http://www.six-sigma.se/FMEA.html`. Visited 13-February-2020.

[17] Tong Wang, Junnan Mi, Zhikai Cai, Xi Chen, and Xiaomin Lian. Vehicle dual-redundancy electronic steering wheel system. *2017 5th International Conference on Mechanical, Automotive and Materials Engineering (CMAME)*, pages 183–187, 2017.

[18] Alejandro D. Dominguez-Garcia, John G. Kassakian, and Joel E. Schindall. A backup system for automotive steer-by-wire, actuated by selective braking. *35th Annual IEEE Power Electronics Specialists Conference*, 2004.

[19] Oliver Rooks, Michael Armbruster, Armin Sulzmann, Gernot Spiegelberg, and Uwe Kiencke. Duo duplex drive-by-wire computer system. *Reliability Engineering & System Safety*, 89(1), 2005.

[20] Henrik Lillberg and Martin Johannesson. Investigation of steering feedback control strategies for steer-by-wire concept, 2018. URL `http://liu.diva-portal.org/smash/record.jsf?pid=diva2%3A1218698&dswid=8121`. Visited 22-January-2020.

[21] Tom Denton. *Automobile Electrical and Electronic Systems*. Routledge, fifth edition, 2017.

[22] Peng Zhang. *Advanced Industrial Control Technology*. William Andrew Publishing, first edition, 2010.

[23] William Bolton. *Mechatronics: Electronic Control Systems in Mechanical and Electrical Engineering*. Pearson, sixth edition, 2015.

[24] dSPACE GmbH. Autobox, 2020. URL https://www.dspace.com/en/ltd/home/products/hw/accessories/autobox.cfm. Visited 03-February-2020.

[25] Vector GmbH. Vn1600, 2020. URL https://www.vector.com/int/en/products/products-a-z/hardware/network-interfaces/vn16xx/. Visited 03-February-2020.

[26] Xuewu Ji, Jingguang Ge, and Hongliang Tian. Reliability improvement of electric power steering system based on iso 26262. *013 International Conference on Quality, Reliability, Risk, Maintenance, and Safety Engineering (QR2MSE)*, 2013.

[27] Julin K Austine and Dr. A.K Parvathy. Practical implementation of four quadrant operation of three phase bldc motor with fuzzy logic controller using fpga. *International Journal of Scientific & Engineering Research*, 5(7), 2014.

[28] Robert Bosch GmbH. Servolectric® torque sensor, 2020. URL https://www.bosch-mobility-solutions.com/en/products-and-services/passenger-cars-and-light-\commercial-vehicles/steering-systems/electric-power-steering-systems/torque-sensor/. Visited 12-February-2020.

[29] Lennart Ljung and Torkel Glad. *Modeling and identification of dynamic systems*. Studentlitteratur, first edition, 2016.